C.P. No. 726

C.P. No. 726

MINISTRY OF AVIATION

AERONAUTICAL RESEARCH COUNCIL

CURRENT PAPERS

Pressure, Heat-Transfer and Temperature Measurements in the Two-Dimensional Nozzle of a Reflected-Shock Tunnel

By

J.L. Stollery, M.Sc. and J.E.G. Townsend, B.Sc.

LONDON: HER MAJESTY'S STATIONERY OFFICE

1964

FIVE SHILLINGS NET

C.P. No.726

Pressure, Heat Transfer and Temperature Measurements in the Two-Dimensional Nozzle of a Reflected-Shock Tunnel

- By -
J. L. Stollery*, M.Sc. and J. E. G. Townsend, B.Sc.

September, 1962

SUMMARY

The flow through the two-dimensional nozzle of a hypersonic reflected shock tunnel was examined experimentally. Schlieren pictures taken with the aid of a Cranz-Schardin apparatus, show the start and development of the nozzle flow. Stagnation point heat-transfer records show the useful tunnel running time and pressure traces give the axial Mach number distribution along the nozzle.

Finally the temperature was measured at two points along the nozzle using the line reversal method. These measurements were difficult to make and must be regarded as preliminary.

List/

---

* This work was undertaken whilst enjoying a six-week vacation consultancy at N.P.L.

Replaces N.P.L. Aero. Report No.1042 - A.R.C.24 159.
Published with the permission of the Director, National Physical Laboratory.

List of Contents

---

1. Introduction

Stagnation temperature measurements made at the nose of a body in a hypersonic wind tunnel using the S.L.R. method[1] have suggested that vibrational freezing occurred in the tunnel nozzle. Subsequent theoretical calculations[2] using experimentally measured vibrational relaxation times confirmed that in all practical hypersonic nozzles non-equilibrium flow will occur with the vibrational energy level freezing at an artificially high level. A simple two-dimensional glass-sided nozzle was therefore designed and fitted to the N.P.L. 3 in. hypersonic shock tunnel so that reversal measurements could be made throughout the nozzle and test section. With helium driving nitrogen the tailoring incident Mach number, M_{s_1} is only 3.4 giving a reflected temperature of 1557°K. Since this is rather low it was decided to operate in the over-tailored condition at $M_{s_1} = 4$. Previous work[3] had shown that steady reservoir conditions $P = 290$ p.s.i.a., $T = 2100$°K would then exist for the period of 1 to 1.6 mS after shock reflection. Calculations showed that the frozen vibrational temperature would be 1950°K.

2. Apparatus

2.1 The shock tunnel

The shock tube and nozzle are shown in Fig. 1. The 3 in. diameter tube has a 14 ft driver section separated from the 18 ft channel by an

unscribed/

unscribed aluminium diaphragm. The second diaphragm held at the nozzle throat by a clamping ring was of 0.00025 in. "Melinex". The 2 in. wide straight-sided nozzle has a divergence semi-angle of 15° and leads to a closed 5 in. test section 2 ft long. The nozzle throat, initially a 0.020 in. slit was later widened to 0.10 in. to raise the density level throughout the measuring area.

For normal operation the channel was evacuated and then filled with nitrogen to 100 mm Hg. The nozzle, test section and dump tank were evacuated to 40μ but owing to leakage the pressure had risen to 150 - 200μ by the time the tunnel was fired. Bottled helium fed to the evacuated chamber burst the first diaphragm naturally, at around 455 p.s.i.a. The incident shock velocity was measured by feeding the signals from two thin film resistance thermometer gauges placed 1 ft apart near the end of the channel to a microsecond counter chronometer.

2.2 Cranz-Schardin equipment[4]

The apparatus, designed by R. J. North at N.P.L. utilised five argon-stabilised sparks which could be fired consecutively at intervals from 2μS upwards. The sequence was triggered from the second of the two thin film gauges mentioned above. The two mirrors used in the Schlieren arrangement were both 12 in. in diameter with focal lengths of 10 and 20 ft respectively.

2.3 Pressure measurements

A quartz SLM PZ-6 transducer was mounted in the end of a 0.4 in. diameter tube 9 in. long mounted axially in the working section from a pedestal mount. The arrangement is shown in Fig. 1. The transducer was coupled via oil filled cable to an SLM PV17 amplifier. The output signal was displayed on a Tetronix 502 oscilloscope and photographed using a Land Polaroid camera.

The gauge was calibrated using a dead weight tester. The calibration curve was perfectly linear over the range 0-300 p.s.i.a.

2.4 Stagnation point heat-transfer rate

A platinum thin film resistance gauge painted across the end of a pyrex rod was mounted in the same way as the pressure transducer. Signals were recorded direct and also after passage through an electronic analogue to give heat-transfer rates immediately. Erosion of the gauge caused by the salt and by aluminium particles from the first diaphragm proved so severe that eventually the thin film was placed off centre. Erosion then virtually ceased.

2.5 Line reversal equipment

Previous very successful S.L.R. temperature measurements behind the incident and reflected shock waves are fully described in Refs. 3 and 5. The apparatus used there was taken over, as was the method of introducing the salt. Brine solution was deposited on a warm coil which was subsequently placed in the side of the channel about 1 ft from the nozzle entrance. The channel was filled with nitrogen then a current of 5 amps passed through the coil. This was sufficient to vaporise the salt and the resultant smoke was drawn through the tube when the channel was sucked down to 100 mm of mercury. Despite the previous success, this method of introducing the salt proved rather unreliable for measurements in the tunnel nozzle. It was impossible to control the salt concentration and for the majority of runs the concentration was inadequate. Other methods of introducing the salt were attempted. Powdered salt was placed in the channel at various positions, powdered salt was rubbed on the end face of the channel, salt was heated in a pyrex tube and the nitrogen drawn over the molten salt into the channel. In general all these attempts resulted in concentrations which were either so low that the resulting signal was swamped by the photomultiplier-background source noise level, or so high that a false absorption signal was recorded. Usable results were obtained by making sufficient runs with the original heater coil technique for introducing the salt.

In the few runs made using chromium carbonyl the compound was introduced in powder form at the end of the channel. The channel was evacuated and held for 30 seconds below 0.25 mm Hg, the vapour pressure of the compound. The channel was then filled with nitrogen to 100 mm Hg.

3. Results

3.1 The nozzle starting process

Two possible wave patterns formed by the nozzle starting process have been discussed by Holder and Schultz in Ref. 6 and are sketched in Fig. 3. Although it was possible to evacuate the nozzle to 40 microns the leak rate was 50 microns per minute so that the tunnel was seldom started against a back pressure less than 150 - 200μ. Under these conditions the flow pattern expected is that shown in Fig. 3b.

To see how rapidly the nozzle started Schlieren pictures were taken at approximately 40 microsecond intervals after shock reflection from the nozzle entry, using the Cranz-Schardin equipment. With the original 0.02 in. throat the density levels in the nozzle were so low that it was very difficult to see even the bow shock around a blunt-ended cylinder mounted in the test section. By widening the throat to 0.1 in. the density level was raised by a factor of five and Fig. 2 shows a sequence of Schlieren pictures taken during two tunnel runs. On frames A and B the first (downstream facing) shock can be seen as a thin convex black line. On picture B both shocks are clearly visible bracketing the nose of the model. Although the flow is supersonic it is difficult to see a bow shock wave. However in the third picture, C, the bow shock is clearly visible with the second starting shock just upstream of it (flow region b, Fig. 3). In frame D the flow seems completely established with the bow shock wrapped around the model. The oblique shocks springing from the nozzle wall change of slope at entry to the parallel test section, are more clearly visible in E.

In most pictures of the nozzle starting process the upstream facing shock was the more clearly visible. From an analysis of 15 runs (75 frames) the passage of this rearmost shock was plotted and is shown in Fig. 4. The first shock was tracked photographically where possible and by measuring the delay on both pressure and heat-transfer records taken at various positions along the nozzle. These results are also shown in Fig. 4. The time interval between the two shocks passing the model station is only 20μS. However, the nozzle starting time, defined as the interval between incident shock reflection at nozzle entry and arrival of the second starting shock at the model, is 150μS. There is a further period required for the establishment of steady flow around the model[6] though when operating the tunnel in the

over-tailored/

over-tailored condition this is usually accomplished by the time the reservoir pressure has reached a steady value.

Extrapolation towards the origin indicates that the starting shocks must decelerate in the first 4 in. of nozzle expansion. The shock velocity is sensibly constant over the rest of the nozzle and Fig. 4 suggests a speeding up once the parallel test section is entered. Using (i) wave speeds suggested by Fig. 4, (ii) nozzle reservoir conditions, P_5 and T_5, measured previously, (iii) the nozzle Mach number deduced from measured pitot pressures, (iv) the simple one-dimensional representation of the starting process shown in Fig. 3, (v) the fact that the nozzle back pressure into which the flow starts lies between 150 and 200μ, then typical theoretical gas flow properties have been calculated and listed on the figure. One point of interest emerges from the figures, namely, the variation of pitot pressure P_0 through the starting process. There is a large increase at the contact surface and a small decrease through the second shock. Thus the starting loads on any model in the working section will be similar to the steady value. The pitot pressure recorded is shown in Fig. 5. The trace is poor because of the gauge "ringing" but during the first 50μS it is possible to see a variation of P_0 that is similar in form, though not necessarily in magnitude, to that suggested in Fig. 3.

3.2 The useful running time

After shock reflection from the end of the channel there are subsequent reflections from both the contact surface and from the tube face as shown in the theoretical x-t diagram of Fig. 6. In practice the contact surface broadens into a mixing region and the reflected shock is re-reflected as a compression fan. Thus from P_5 upwards compression is accomplished gradually rather than in discrete steps. Previous measurements[3] had shown that the reservoir pressure reached a steady level between 1 and 2 mS after the first shock reflection and that during this period the temperature reached its maximum value of 2100°K. Fig. 7 compares the theoretical and experimental pressure and temperature histories. Both the reduction in P_8 and the drop in temperature are probably due to attenuation of the reflected shock resulting from interaction with the boundary layer as discussed in Ref. 6. It is important to note that whilst the pressure subsequently rises close to the "equilibrium interface" value[6,7] the temperature does not increase. In fact it decays at a rate of approximately 50°K per millisecond. This throws serious doubt on the ability of the equilibrium interface technique for increasing the reservoir enthalpy as suggested in Ref. 7.

For the purposes of SLR measurements the higher the temperature the greater the signal to noise ratio for any given degree of temperature mismatch. The 'useful' running time was therefore the period 0 to 2 mS which included two separate periods when the reservoir temperature and pressure were sensibly constant. Stagnation point transfer records taken in the nozzle also showed two 'steady' periods within the first two milliseconds of flow. Fig. 8 shows the stagnation point heat-transfer rate in the lower trace which was obtained directly from the surface temperature measurement in the upper trace using an electrical analogue.

For other types of measurement it would no doubt be an advantage to use the longer cooler steady flow period that occurs later in the run between 4 and 8 mS from the start.

3.3 The pressure distribution along the nozzle axis

The steady pitot pressure recorded (during the time interval 1-2 mS described above) at various points along the axis of the nozzle is compared with one-dimensional theory in Fig. 10. Both the frozen[8] and equilibrium[9] pitot pressures were calculated and proved to be virtually identical if plotted against nozzle area ratio. Despite the fact that the real flow is neither one-dimensional nor inviscid the theory gives a reasonable picture of the pressure distribution along the nozzle. The difference between the calculated frozen and equilibrium static pressures amounted to 13% in the working section and in any future investigation it would be worthwhile attempting to measure these pressures.

At all stations along the nozzle the variation of pitot pressure with time is very similar to a scaled down reproduction of the reservoir pressure history. The comparison is made in Fig. 9. The rapid decrease in pressure after 8 mS is caused by the reflected head of the expansion fan propagating through the nozzle. However, Schlieren pictures taken 15 mS after the start still show flow, by now much cooler and at lower pressure, fully established in the working section.

3.4 Analysis of the SLR results

Measurements were attempted at two stations along the nozzle axis, namely, 7 in. and 15 in. from the throat. A double beam technique was used, each beam lying at 15° to the normal as shown in Fig. 1. Separate "Pointolite" background sources were employed. Owing to the difficulties of salt distribution the strength of signal varied greatly from run to run. Fig. 11a shows the best trace obtained at the 7 in. station with both signals indicating emission relative to background source temperatures of 1600°K and 1800°K. Extrapolating linearly the temperature history can be calculated and is shown in Fig. 11b. As might be hoped it bears a striking resemblance to the reservoir temperature record which is included in the figure for comparison. The tentative conclusion is that at this position in the nozzle where the translational temperature is approximately 300°K, the vibrational temperature is frozen at 1900°K.

Many of the signals recorded were too small to justify interpolation or extrapolation but showed whether the gas was in absorption or emission. Fig. 12 collects the usable results and confirms the value of 1900°K given above. The similar picture for the 15 in. station is shown in Fig. 13. It was found impossible to obtain useful signals if the mismatch between source temperature and gas temperature was less than 200°K. The only conclusion was that at this nozzle position the vibrational temperature lay between 1700 and 2100°K.

The value of 1900°K measured at the 7 in. station compares very favourably with the theoretical value of 1950°K calculated using Ref. 2.

The theoretical distribution of vibrational temperature, shown in Fig. 14, demonstrates that freezing occurs just downstream of the nozzle throat.

4. Conclusions

1. Electronically-excited sodium atoms have a radiative lifetime of 10^{-8} seconds which is very small in comparison with the nozzle flow

transit/

transit time. There is therefore no question of such atoms being convected downstream in a state dictated by the reservoir conditions.

2. The vibrational energy of the gas freezes at a level similar to that predicted by a simple one-dimensional flow analysis.

3. The nozzle started in 150μS against a back pressure of 200μ. The starting shock system closely resembles the 1-D model discussed in Ref. 6.

4. A much better method of introducing sodium atoms into the nozzle flow is needed. If this could be found then it would be very interesting to alter the reservoir conditions and/or nozzle geometry so that freezing occurred further downstream, within the glass-walled temperature measuring section.

5. Acknowledgements

The authors gratefully acknowledge the generous help of many people at the N.P.L. In particular we wish to thank Dr. Lapworth, Dr. Pennelegion, Mr. North and Mr. Busing and also the N.P.L. workshop staff. Without their assistance the experimental programme could not possibly have been carried out in the limited time available.

6. Postscript

Further work at N.P.L. by Lapworth and Townsend has shown the danger of radiation from the reservoir gas passing through the nozzle throat, scattering from the nozzle side walls and entering the photomultiplier tube. It is clear that much more needs to be done before really reliable results for the distribution of vibrational temperature through a nozzle can be obtained.

7. List of Symbols

a	sound speed
P	pressure
P_o	pitot pressure
ρ	density
T	temperature
u	flow velocity
U	wave velocity
M	Mach number
M_{s_1}	incident shock Mach number $= U_{s_1}/a_1$
x	distance along the shock tube
ξ	distance along the nozzle measured positive downstream from the throat
t	time.

For other notation and suffices see Figs. 3, 6 and 7.

References/

References

No.	Author(s)	Title, etc.
1	J. L. Stollery	Stagnation temperature measurements in a hypersonic gun tunnel using the sodium line reversal method. Imperial College of Science and Technology. Aeronautics Department Report No.16, September, 1960. A.R.C.22,854. May, 1961. See also "Nature", Vol.190, pp.778-779, May 27, 1961.
2	J. L. Stollery and J. E. Smith	A note on the variation of vibrational temperature along a nozzle. J.F.M., Vol.13, pp.225-236, 1962.
3	K. C. Lapworth and J. E. G. Townsend	Reservoir temperature measurements in a hypersonic shock tunnel by sodium line reversal. Part 2 - Double beam method. To be published.
4	R. J. North	High-speed photography applied to high-speed aerodynamic research. Proc. 5th International Congress on High-Speed Photography. Washington 1960.
5	K. C. Lapworth, J. E. G. Townsend and K. Bridgeman	Reservoir temperature measurements in a hypersonic shock tunnel by sodium line reversal. Part 1 - Single beam method. A.R.C.23,341. December, 1961.
6	D. W. Holder and D. L. Schultz	The duration and properties of the flow in a hypersonic shock tunnel. Progress in Astronautics and Rocketry - Vol.7, Hypersonic Flow Research. Academic Press 1962.
7	J. A. Copper	Experimental investigation of the equilibrium interface technique. Physics of Fluids, Vol.5, pp.844-849, July 1962.
8	Ames Research Staff	Equations, tables and charts for compressible flow. N.A.C.A. Report 1135, 1953.
9	L. Bernstein	Equilibrium real-gas performance charts for a hypersonic shock-tube wind-tunnel employing nitrogen. A.R.C. C.P.633, September, 1961.

10/

No.	Author(s)	Title, etc.
10	L. Bernstein	Tabulated solutions of the equilibrium gas properties behind the incident and reflected normal shock-wave in a shock-tube. I. Nitrogen. II. Oxygen. A.R.C. C.P. No.626, April, 1961.

ES

FIG. 1

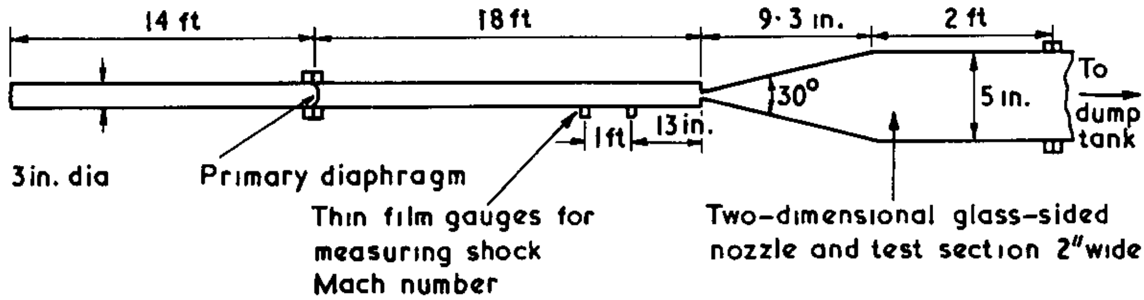

(a) General arrangement of the 3" shock tunnel

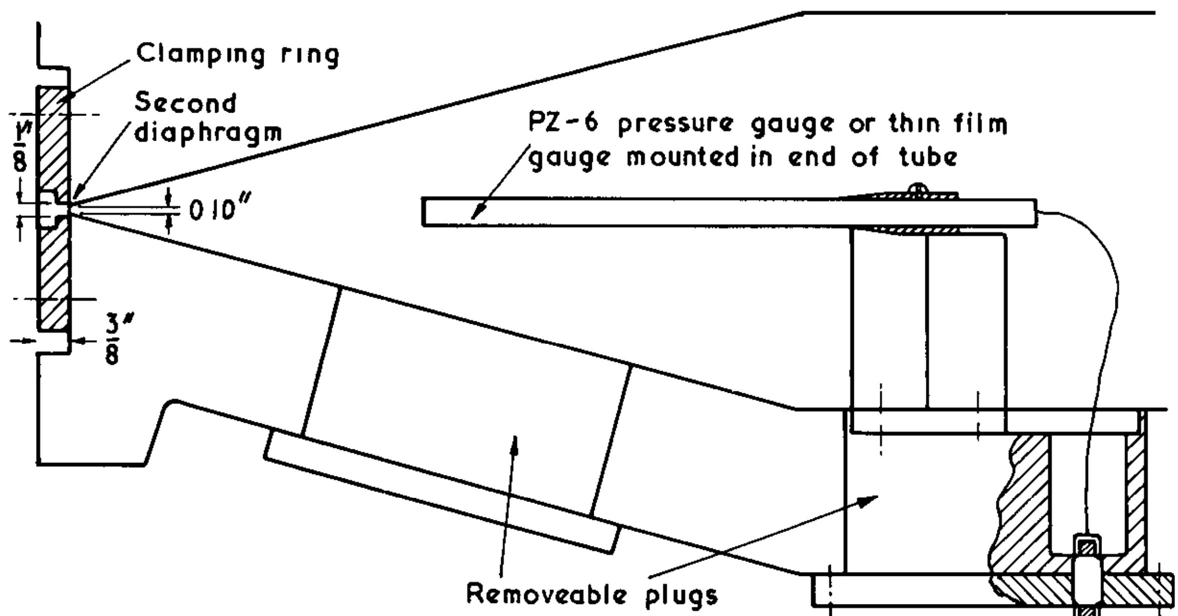

(b) Details of nozzle and mount for pressure and heat transfer transducers.

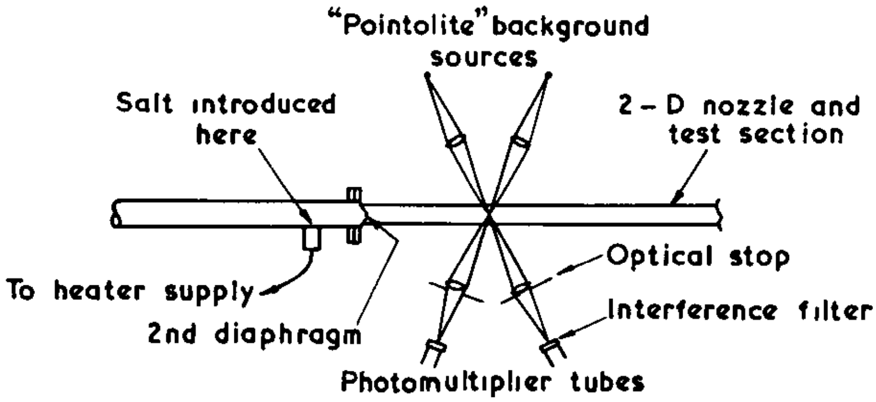

(c) Details of arrangement for S.L.R. measurements

FIG. 2

A

Run 35 frame 2, t = 74 μS

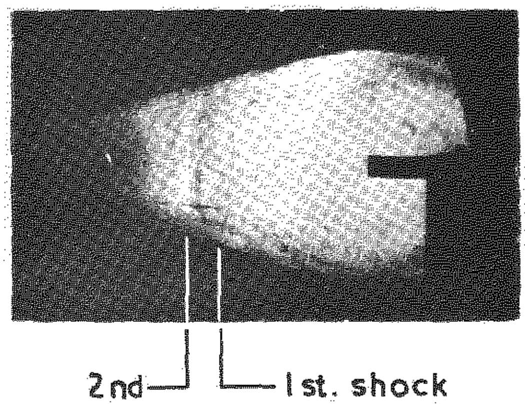

B

Run 36 frame 3, t = 124 μS

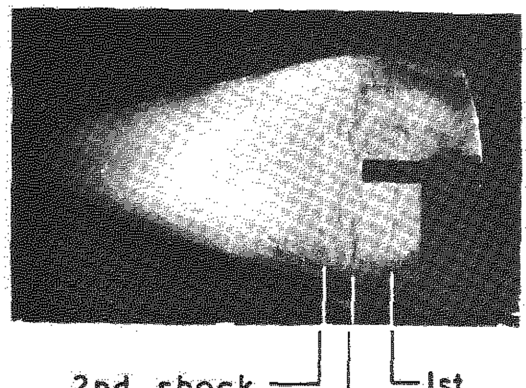

C

Run 35 frame 3, t = 134 μS

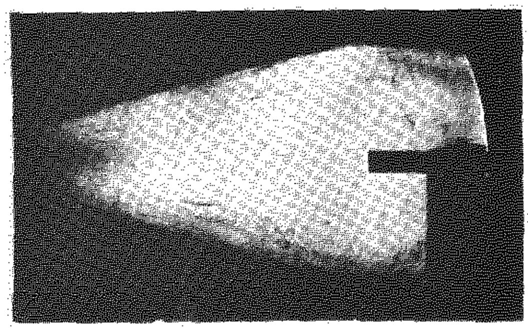

First sign of supersonic flow relative to the probe in the test section

D

Run 36 frame 4, t = 200 μS

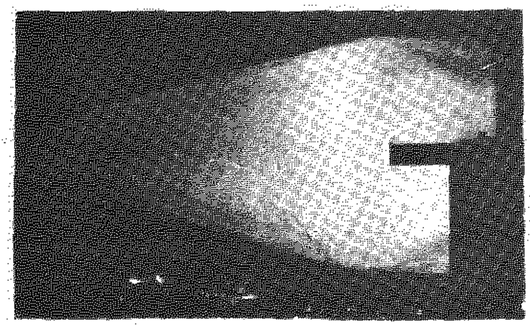

Flow established around the probe.

E

Run 36 frame 5, t = 1200 μS

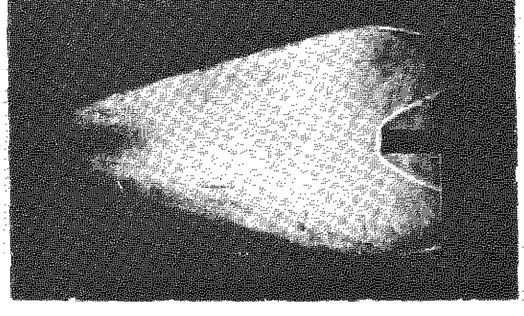

Schlieren pictures showing the flow starting process

FIG. 3

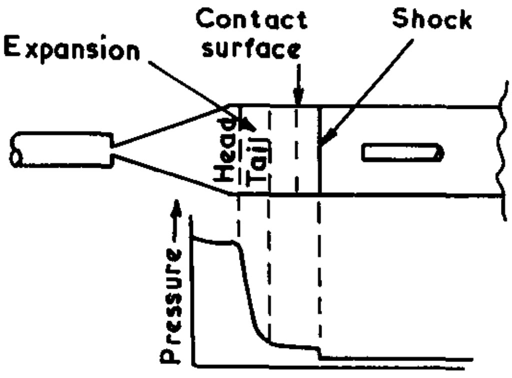

(a) Low initial pressure in working section

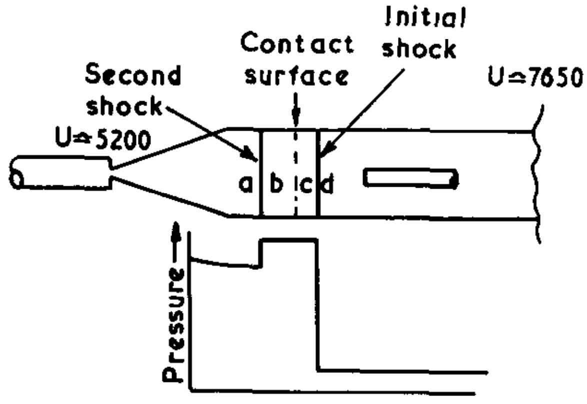

(b) High initial pressure in working section

Typical values of the flow properties

		a	b	c	d
P	psia	0·153	0·191	0·191	0·0036 = 188 μ
T	°K	263	281	2830	292
$10^6 \rho$	slugs/cu.ft	26·2	30·9	2·97	0·55
u	ft/sec	6400	6220	6220	0
P_0	psia	6·95	7·7	0·85	0·0036
M	—	5·91	5·56	1·75	0

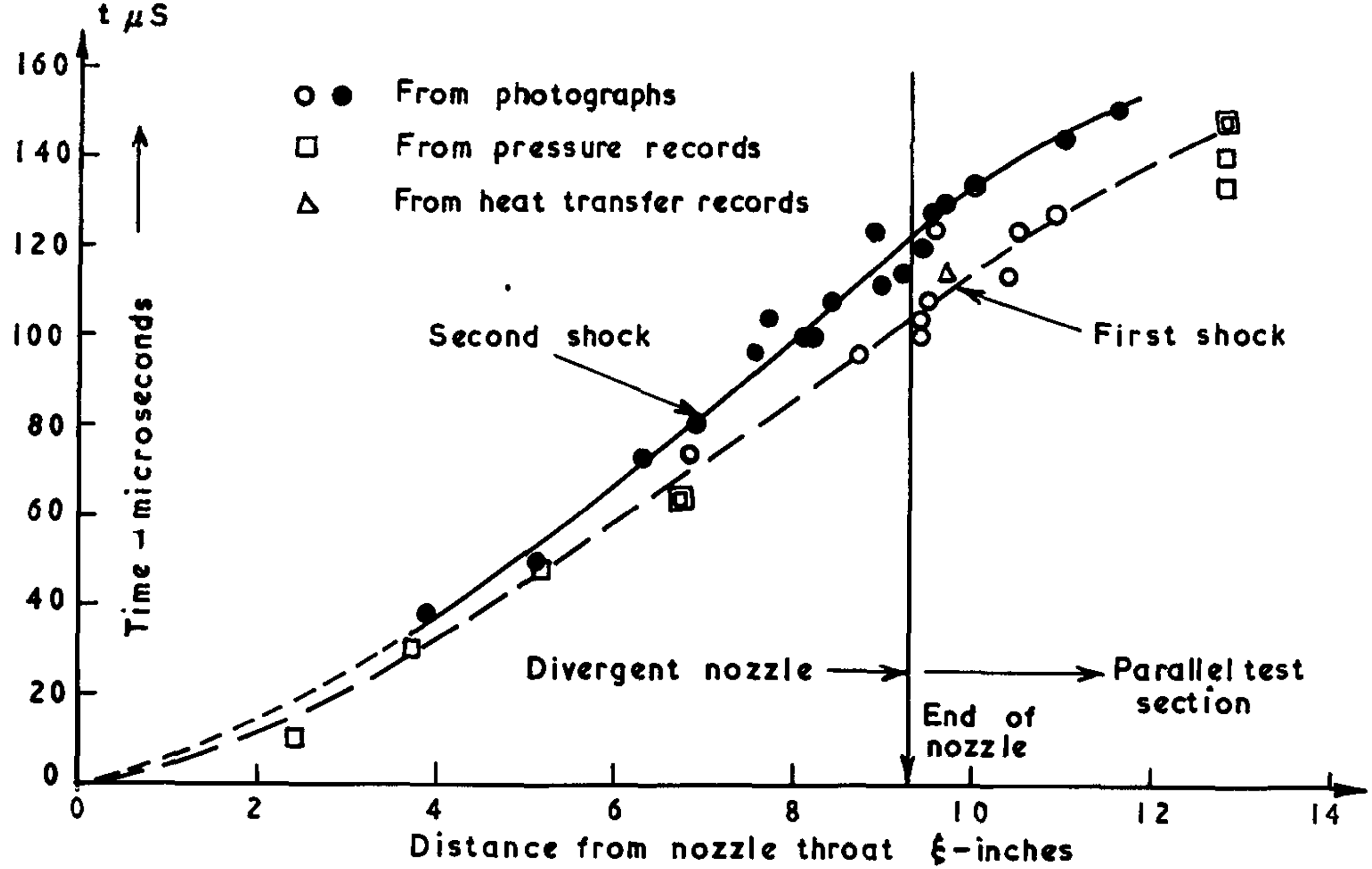

FIG.4

Passage of starting shock system through the nozzle

FIG. 5

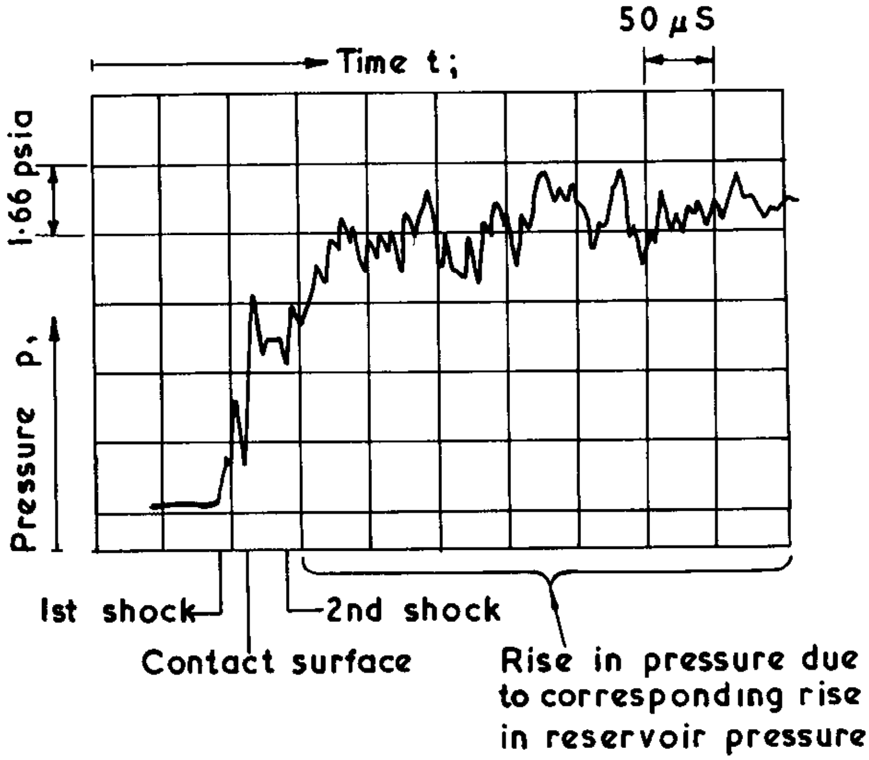

Run 119 Pitot pressure trace showing the start of flow in the test section, $\xi = 12{\cdot}8''$

FIG. 6

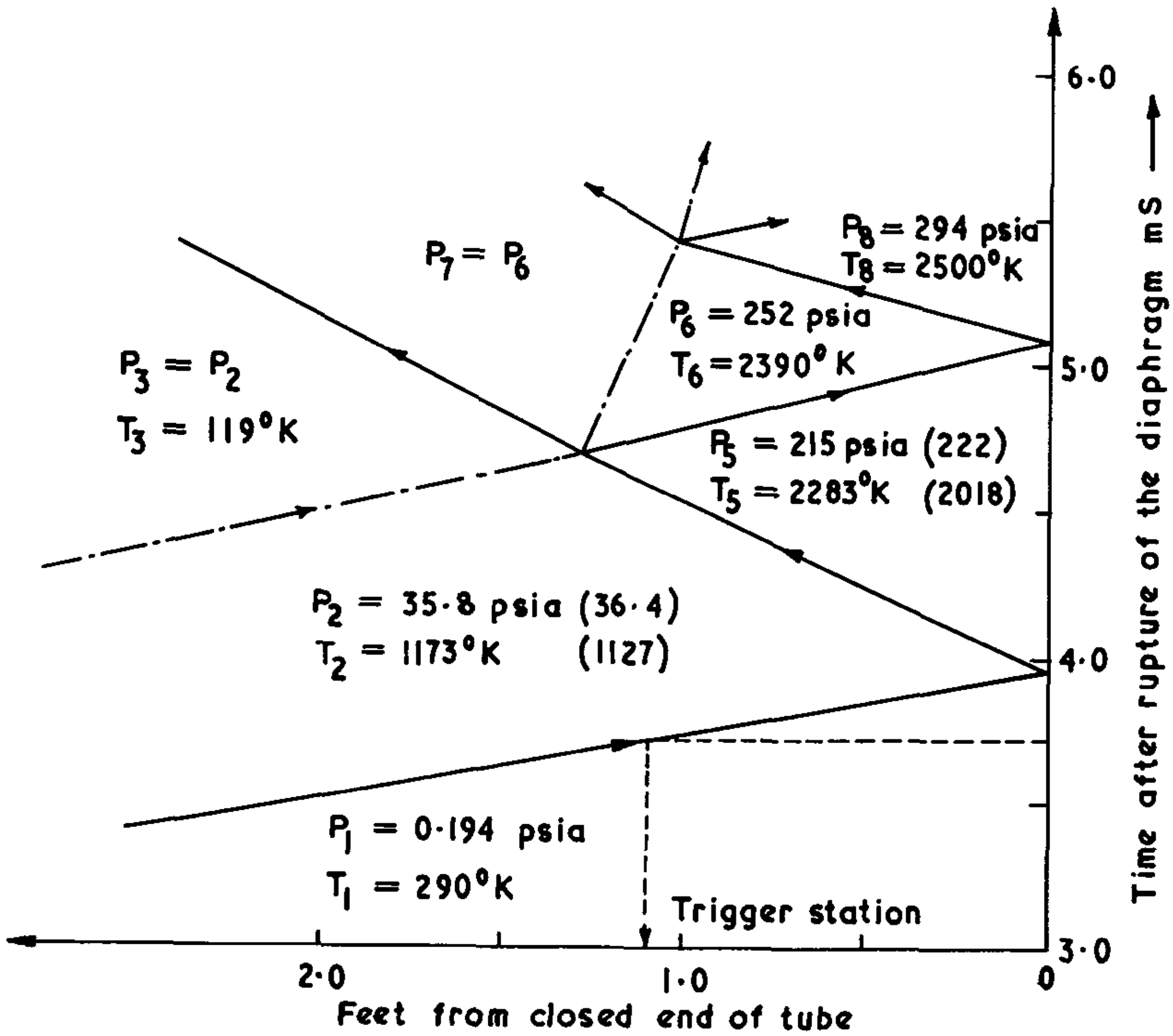

Theoretical wave diagram for $M_{S_1} = 4·0$

(Numbers in brackets refer to eq^m real gas values)

FIG. 7

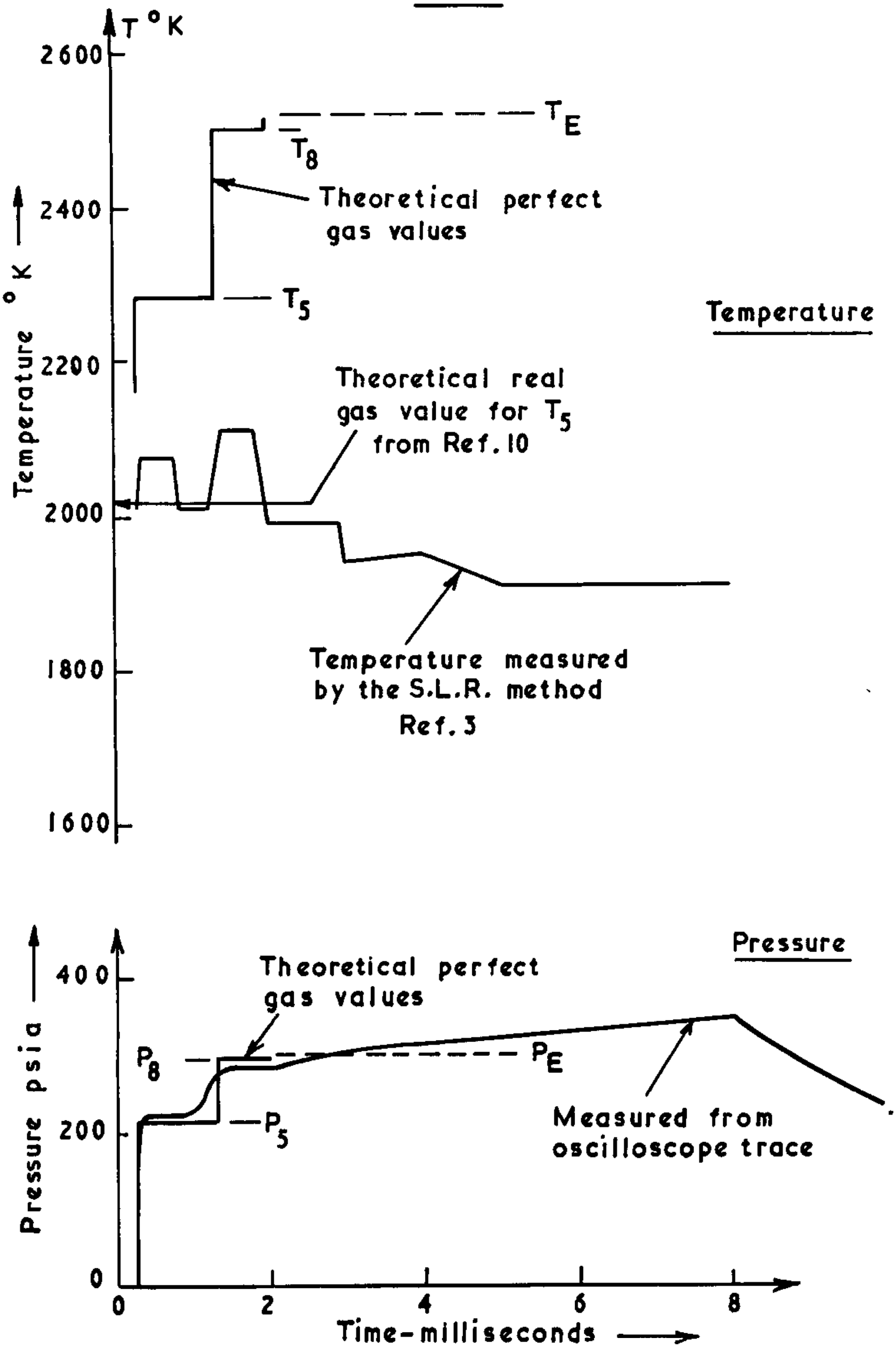

Comparison between theoretical and experimental reservoir conditions $M_{s_1} = 4 \cdot 0$

FIG.8.

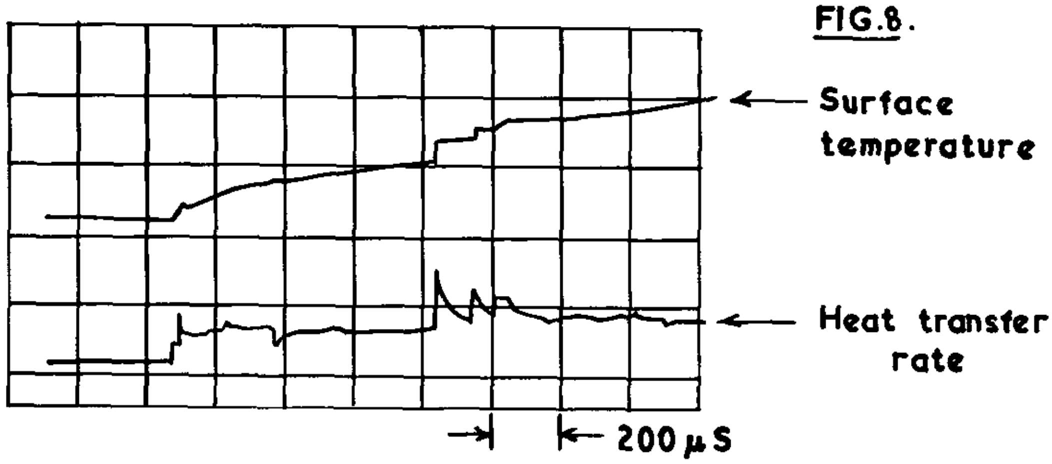

Run 129. Record from a stagnation point thin film platinum resistance gauge mounted in the test section, $\xi = 12 \cdot 8''$

FIG. 9(a)

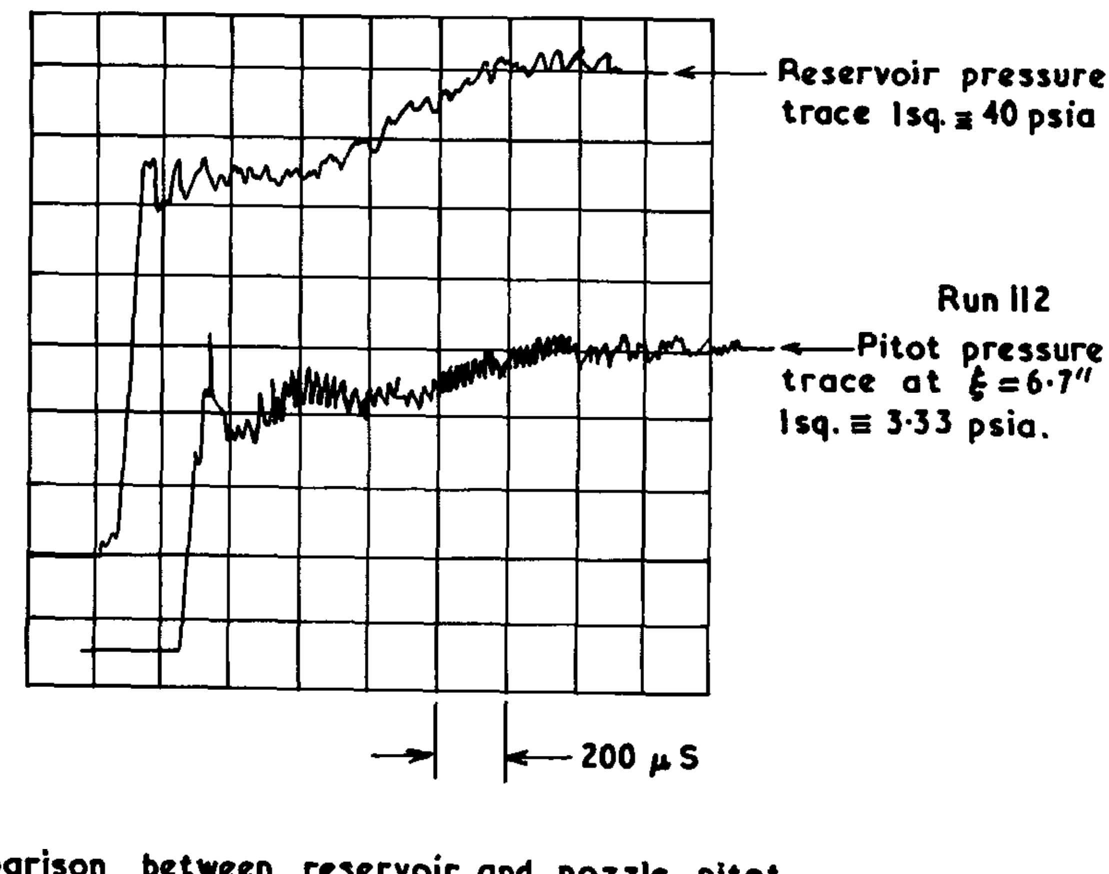

Comparison between reservoir and nozzle pitot pressure histories.

FIG 9b

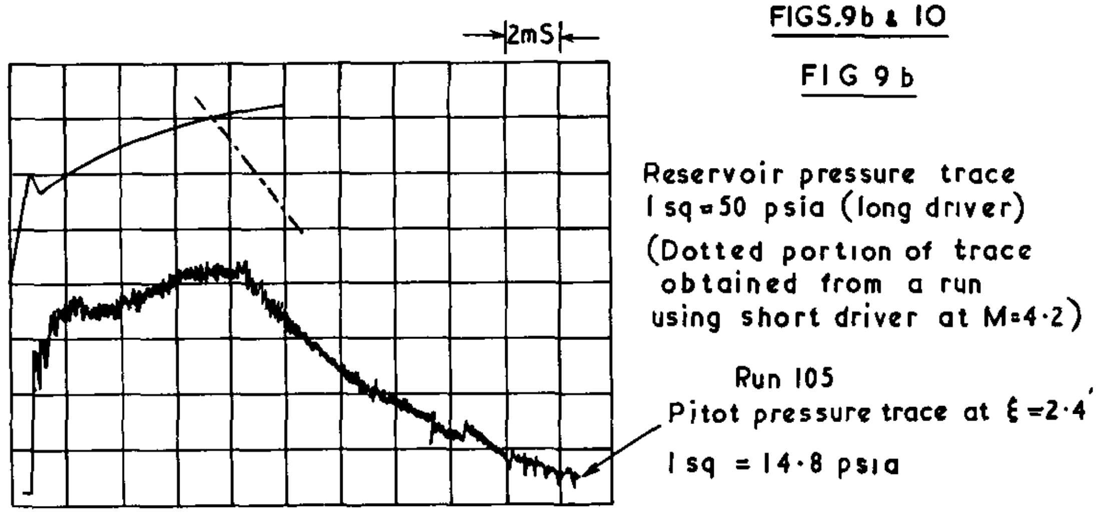

Comparison between reservoir and nozzle pitot pressure histories

FIG 10

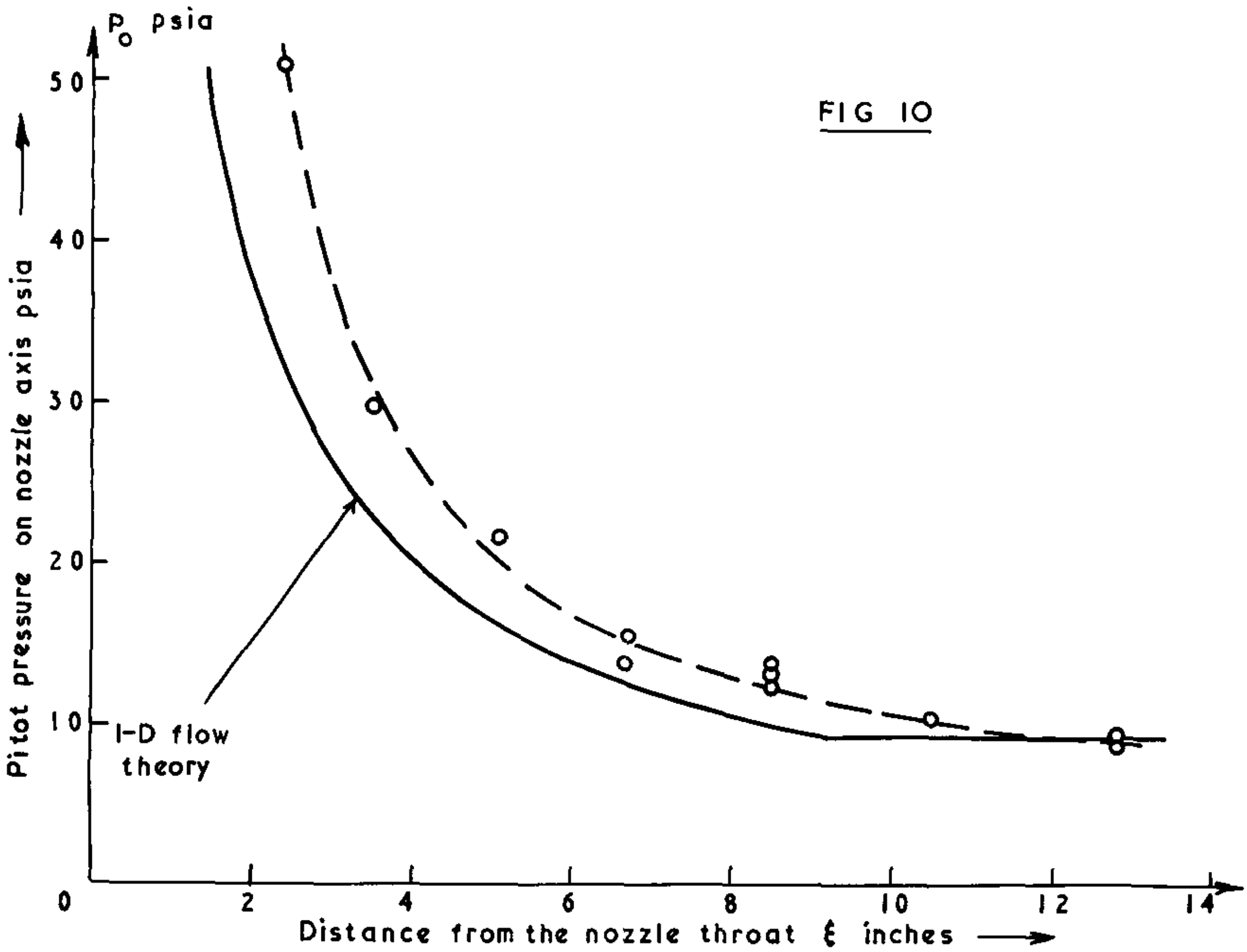

Comparison between the measured pressure distribution along the nozzle axis and 1-D theory.

FIG. 11 (a & b)

FIG. 11(a)

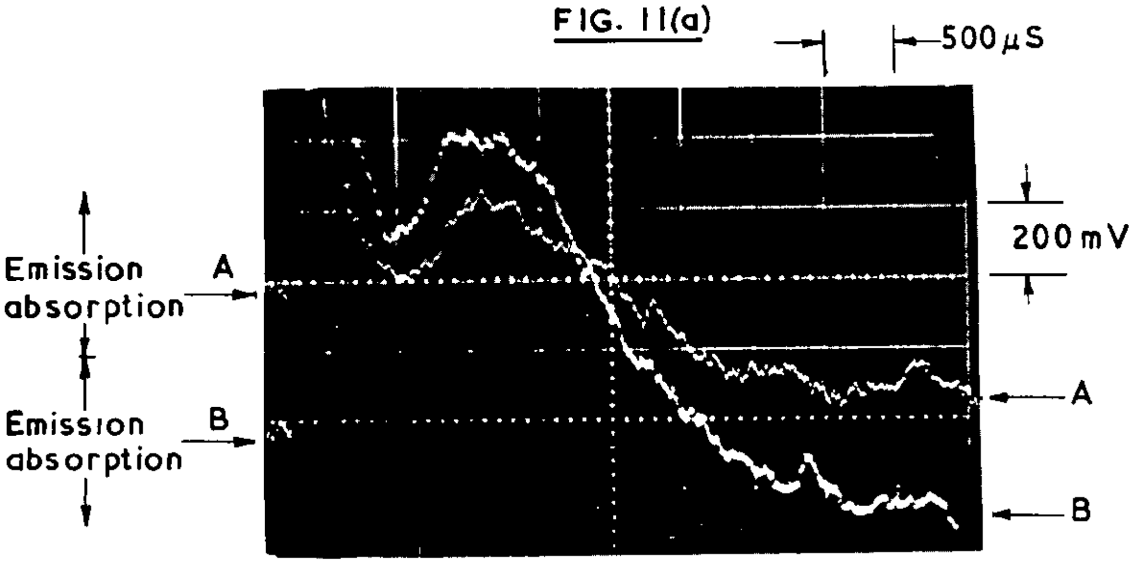

Run 58. S.L.R. record with background source temperatures $T_A = 1800°K$, $T_B = 1600°K$

FIG. 11(b)

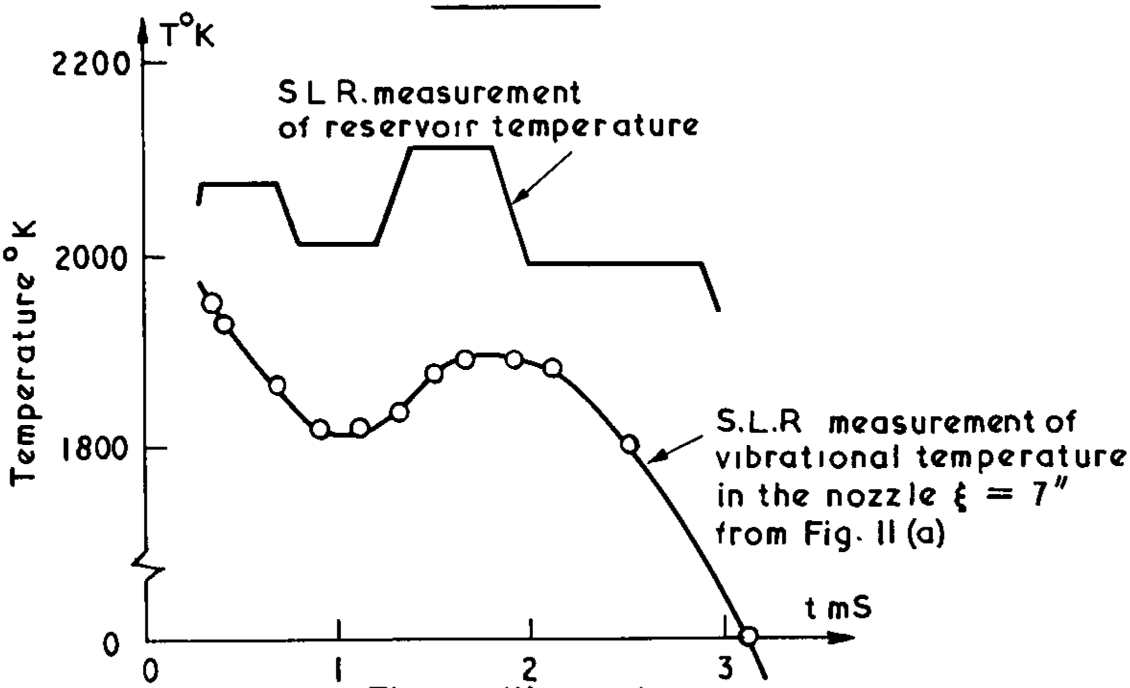

Comparison between nozzle and reservoir measurements using the S.L.R. method

FIGS. 12 & 13.

FIG. 12.

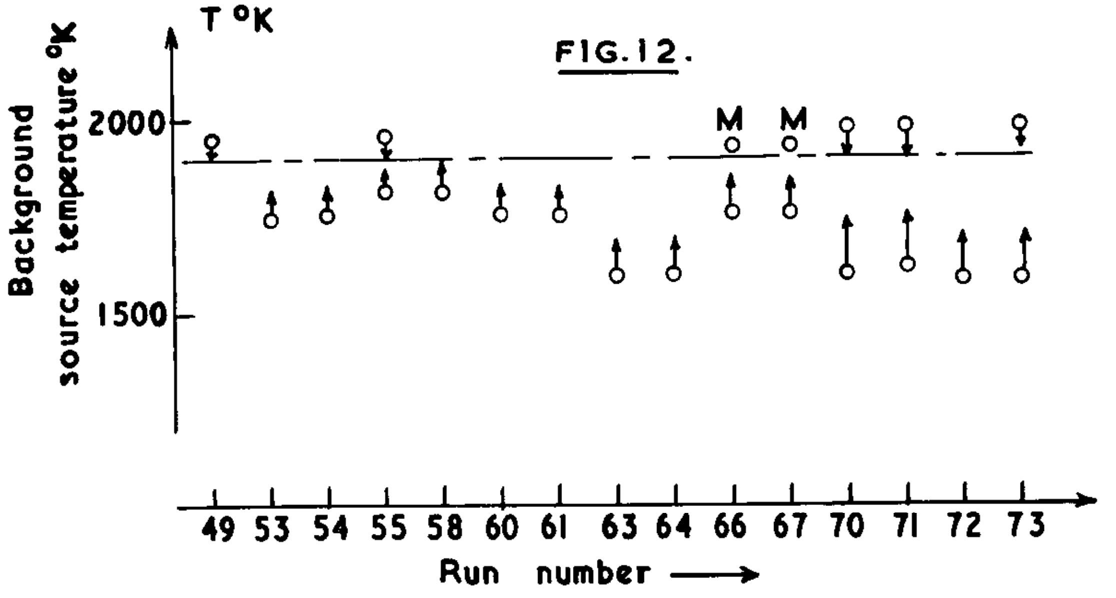

Analysis of S.L.R. results at $\xi = 7''$. Arrows indicate the direction in which the source temperature should be changed to obtain a match. A letter M over a point denotes a close match.

FIG. 13.

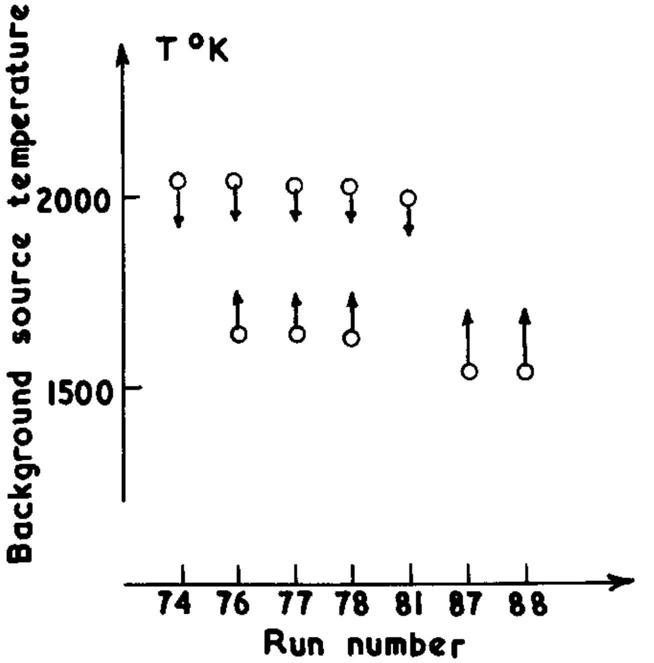

Analysis of S.L.R. results at $\xi = 15''$

D 7780/Wt.60 K.5 8/64 XL & CL

FIG. 14.

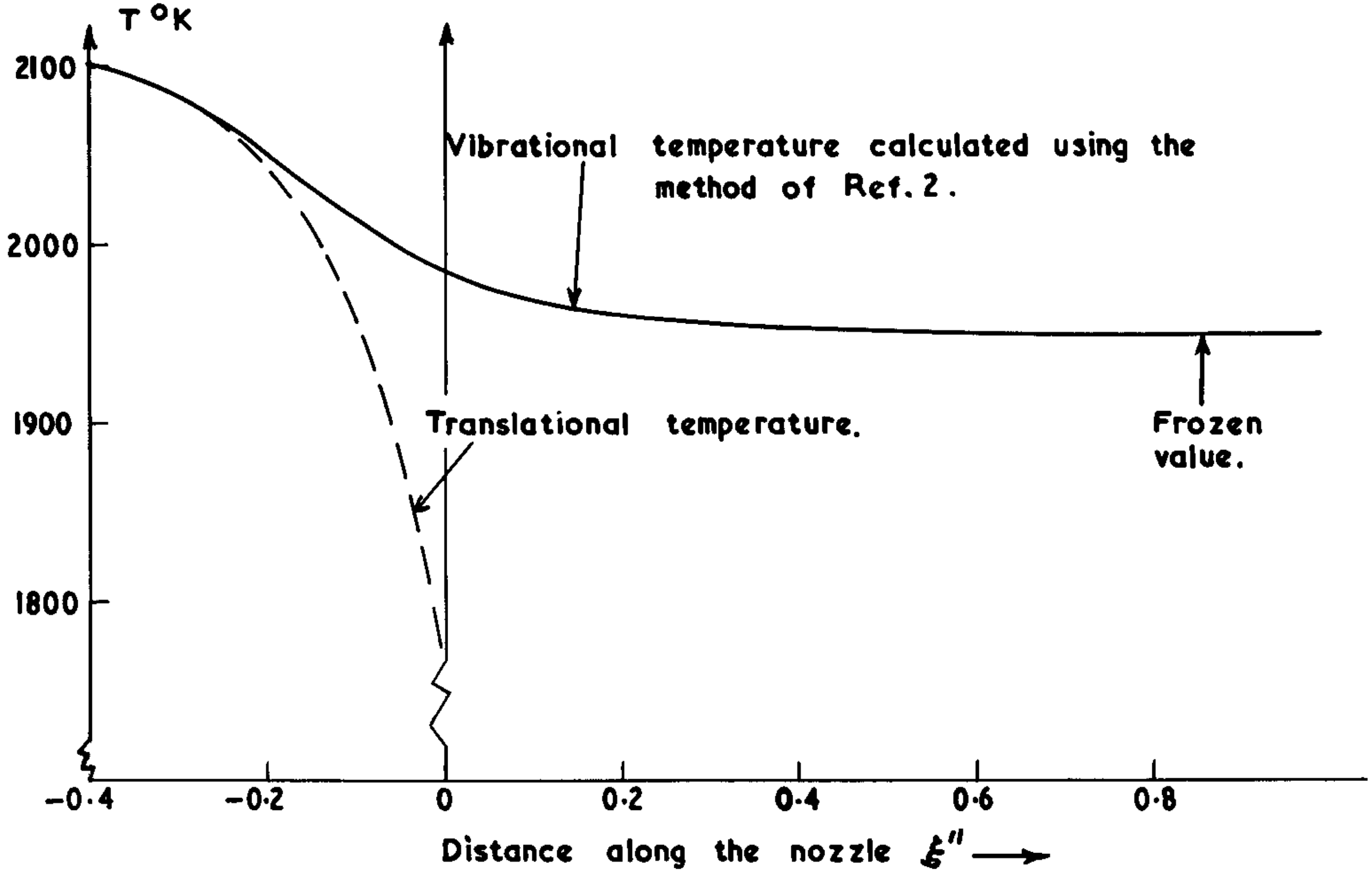

Théoretical distribution of vibrational temperature along the nozzle.

A.R.C. C.P. No.726
September, 1962
Stollery, J. L. and Townsend, J. E. G.

PRESSURE, HEAT-TRANSFER AND TEMPERATURE MEASUREMENTS IN THE TWO-DIMENSIONAL NOZZLE OF A REFLECTED-SHOCK TUNNEL

Cranz-Schardin Schlieren pictures were taken of the development of the nozzle flow in a two-dimensional working section. Stagnation point heat-transfer and pressure records show useful running time and axial Mach number distribution.

Temperature was measured at two points using the line reversal method. The results indicate that the vibrational energy freezes as theory suggests.

A.R.C. C.P. No.726
September, 1962
Stollery, J. L. and Townsend, J. E. G.

PRESSURE, HEAT-TRANSFER AND TEMPERATURE MEASUREMENTS IN THE TWO-DIMENSIONAL NOZZLE OF A REFLECTED-SHOCK TUNNEL

Cranz-Schardin Schlieren pictures were taken of the development of the nozzle flow in a two-dimensional working section. Stagnation point heat-transfer and pressure records show useful running time and axial Mach number distribution.

Temperature was measured at two points using the line reversal method. The results indicate that the vibrational energy freezes as theory suggests.

A.R.C. C.P. No.726
September, 1962
Stollery, J. L. and Townsend, J. E. G.

PRESSURE, HEAT-TRANSFER AND TEMPERATURE MEASUREMENTS IN THE TWO-DIMENSIONAL NOZZLE OF A REFLECTED-SHOCK TUNNEL

Cranz-Schardin Schlieren pictures were taken of the development of the nozzle flow in a two-dimensional working section. Stagnation point heat-transfer and pressure records show useful running time and axial Mach number distribution.

Temperature was measured at two points using the line reversal method. The results indicate that the vibrational energy freezes as theory suggests.

C.P. No. 726

Printed and published by
HER MAJESTY'S STATIONERY OFFICE
To be purchased from
York House, Kingsway, London W C 2
423 Oxford Street, London W.1
13A Castle Street, Edinburgh 2
109 St Mary Street, Cardiff
39 King Street, Manchester 2
50 Fairfax Street, Bristol 1
35 Smallbrook, Ringway, Birmingham 5
80 Chichester Street, Belfast 1
or through any bookseller

Printed in England

C.P. No. 726

S.O. Code No 23-9015-26